Conditions for Laminar Flow in Geophysical Vortices

BRIAN H. FIEDLER

Department of Mathematics, Monash University, Clayton, Victoria, Australia

(Manuscript received 3 March 1988, in final form 1 August 1988)

ABSTRACT

The sufficient condition for inviscid, helical instability at large wavenumbers is applied to solutions for columnar vortices arising from the vortical flow of an end-wall boundary layer. The end-wall vortex arising from the laminar boundary layer under a potential vortex will be unstable at sufficiently high Reynolds number. However, if the end-wall boundary layer is turbulent, the end-wall vortex can be stable and laminar even at very high Reynolds number; therefore, stable, laminar tornadoes and waterspouts are suggested as theoretical possibilities.

1. Introduction

Columnar vortices perpendicular to a stationary end-wall may have a core of confined vorticity in which the fluid is continually swept in from the end-wall boundary layer. Using the solution of Burggraf et al. (1971) for the boundary layer under a potential vortex, Fiedler and Rotunno (1986; hereafter FR) solve for the structure of the end-wall vortex. For large values of Reynolds number Re, the radius of the core (radius of maximum azimuthal speed) is about equal to the terminal depth δ of the boundary layer where

$$\delta \equiv \left(\frac{\nu}{\Gamma_0}\right)^{1/2} R \equiv \mathrm{Re}^{-1/2} R, \tag{1.1}$$

ν is the viscosity, Γ_0 the circulation in the potential vortex, and R the radius at which the boundary layer begins forming. In the limit $\mathrm{Re} \to \infty$, the vortical fluid, although having lost circulation by friction in the end-wall boundary layer, will be loss-free in the sense that its stagnation pressure will be the same as that of the flow external to the core. With pressure falling monotonically towards the axis and radial and azimuthal velocity being zero on the axis, an axial jet will therefore exist in the core. Fiedler and Rotunno (1986) show that in theory, as in experiment, the loss-free, end-wall vortex has a maximum axial velocity about twice the maximum azimuthal velocity.

The axial jet renders such a vortex supercritical with respect to centrifugal waves and the vortex can maintain a large dynamic pressure drop in the core despite a smaller pressure drop existing downstream. Coupling to downstream conditions would occur via a vortex breakdown. The flow downstream of the vortex breakdown is usually more turbulent than the upstream flow though, as Leibovich (1984) points out, the observed instability in the downstream flow is not necessarily the cause of the breakdown. Furthermore, vortex breakdown is not a necessary precursor for turbulence in the core; the supercritical flow upstream of the breakdown can be either laminar or turbulent. This paper is concerned with the conditions for a transition to turbulence in supercritical vortices without a vortex breakdown. A primary motivation is to understand how supercritical tornadoes and waterspouts (if they do exist) can remain stable even at very high Reynolds number. The work of Leibovich and Stewartson (1983; hereafter, LS) seems to indicate that supercritical end-wall vortices formed at high Reynolds number should be unstable as a result of the axial jet. The distinct concepts of criticality and stability are thoroughly discussed in Leibovich (1984).

Many experimental columnar vortices are apparently well modeled by the so-called Q-vortex with dimensionless radial profiles of axial vorticity ζ and axial velocity W given by

$$\zeta(r) = 2qe^{-r^2} \tag{1.2a}$$

$$W(r) = e^{-r^2} + W_\infty \tag{1.2b}$$

where q and W_∞ are constants. Leibovich and Stewartson quote experiments for which these bell-shaped profiles appear to fit the measurements and they and others find the Q-vortex convenient for stability studies.

An end-wall vortex is assumed here to be modeled closely by $W_\infty = 0$. Experiments (e.g., Phillips and Khoo 1987) have shown that end-wall vortices can become essentially columnar with a distance of a few δ downstream from the end-wall. This analysis is restricted to situations where—at least within a radius of a few δ and within a few δ from the end-wall—the

Corresponding author address: Dr. Brian H. Fiedler, School of Meteorology, University of Oklahoma, 200 Felgar St., Room 219, Norman, OK 73019.

meridional flow external to the vortical flow is relatively weak. The approximation $W_\infty = 0$ is clearly reasonable for the experiment profiles shown in Phillips and Khoo (1987). The approximation is also justifiable at least for the narrower tornadoes and waterspouts when applied within a few tens of meters from the surface, where any convective updraft external to the core would be weak.

A loss-free, end-wall vortex is closely modeled by $W_\infty = 0$ and $q = 0.86$ (see section 3). However, the relatively large axial velocity in such a vortex that leads to supercriticality and the prevention of turbulence via vortex breakdown also leads to inertial instability due to the shear in the axial flow. In fact, LS show that for $q < 1.41$, a Q-vortex is unstable to large-wavenumber, helical modes. For $q = 0.86$, the most unstable mode has an e-folding time of 2.2. For $W_\infty = 0$, the Q-vortex is subcritical for *any* $q \neq 0$. This subcriticality can be an artifact of the representation of the profiles at large r; if $W_\infty > 0.018$, then the flow is supercritical for $q = 0.86$. However, in a stable vortex with $q > 1.41$, supercriticality occurs only with $W_\infty > 0.20$. Therefore, stable Q-vortices with $W_\infty = 0$ are fundamentally subcritical because the core itself allows waves to propagate upstream. Thus, stability theory applied to (1.2) seems to imply that stable, supercritical, end-wall vortices are not likely to exist, be they loss-free or otherwise.

Stable, supercritical end-wall vortices have, of course, been observed (e.g., see the picture in FR). The characteristics of viscosity suggest that it itself is a reason for the observed stability to large-wavenumber modes. However, despite the fact that the core becomes smaller with increasing Re, the dimensionless diffusion time scale is easily shown to be n^{-2} Re. Leibovich and Stewartson (1983) find that the large-wavenumber limit of the growth rate is approached within 3% when azimuthal wavenumber $n = 3$. Considering the example with $q = 0.86$, the damping of a helical instability by viscosity should be insignificant except for Re $\leqslant$ 1000. Lessen and Paillet (1974) find that complete stabilization for $q = 0.86$ would occur only with Re $\leqslant$ 20. The effect of viscosity on the mean state also decreases with increasing Re despite the fact that δ becomes smaller. The core is advected downstream a dimensional length proportional to $\mathrm{Re}^{1/2}R$ before viscous effects become significant. A quick calculation using dimensions and velocities of a narrow waterspout or tornado will show that the core is easily advected through the depth of the troposphere, without the mean state or a helical instability suffering significant diffusion by molecular viscosity.

In this paper I show how end-wall vortices can be both supercritical and stable to all inviscid large-wavenumber helical modes, two-dimensional modes, and axisymmetric modes. The derived vortex profiles are bell shaped and only subtly different from the vortex that would erupt axially from the end-wall boundary-layer solution of Burggraf et al. (1971) as Re $\rightarrow \infty$ (hereafter referred to as the loss-free Burggraf boundary layer). This latter vortex (hereafter referred to as the loss-free Burggraf vortex) was shown to be unstable in FR. I show that if a loss-free, end-wall vortex is to be stable, then the circulation in the boundary layer must approach asymptotically the external value less rapidly with height than it does in the loss-free Burggraf boundary layer. Alternatively, the end-wall vortex could be stable only if sufficient loss of head occurred in the end-wall boundary layer, as would be the case if Re were sufficiently small or if the end-wall boundary layer were turbulent.

2. Large-wavenumber helical instability

Below, I present a heuristic derivation of the growth rate of the large-wavenumber helical modes that to my knowledge has not been published before. The derivation will take a different approach from that of Emanuel (1984), which emphasizes the isomorphism to the larger scale inertial instability familiar to meteorologists. As in LS, I assume that an incompressible fluid filling all space has velocity vector $(0, V(r), W(r))$ where r is the radial coordinate in a cylindrical (r, θ, z) coordinate system. The perturbation velocity and pressure are assumed to be of the form

$$(u', v', w', p'/\rho) = (u(r), v(r), w(r), \sigma(r)) \times \exp[i(\alpha z - n\theta - \omega t)]. \quad (2.1)$$

The perturbation radial momentum equation [e.g., Drazin and Reid (1982), p. 74] is

$$i(-\omega - \Omega n + W\alpha)u - 2\Omega v = -D\sigma \quad (2.2)$$

where $\Omega \equiv V/r$ and $D(\ ) \equiv d(\ )/dr$. The perturbation radial vorticity equation is

$$i(-\omega - \Omega n + W\alpha)\left(\alpha v + \frac{n}{r}w\right) + \frac{1}{r}D\Gamma\alpha u + DW\frac{n}{r}u = 0, \quad (2.3)$$

where $\Gamma = rV$. The last two terms represent generation of perturbation radial vorticity by tilting mean vertical vorticity and mean azimuthal vorticity. The continuity equation is

$$\frac{1}{r}D(ru) + i\alpha w - i\frac{n}{r}v = 0. \quad (2.4)$$

The analysis here is restricted to normal modes which at some radius $r = r_0$ have a length scale of radial variation which is much larger than that of vertical and azimuthal variation. The perturbation velocity components are all assumed to be of the same order. Therefore, the first term in (2.4) is neglected. After obtaining a perturbation pressure scale from the vertical or azimuthal momentum equation, the radial pressure gradient in (2.2) can be shown to be an order smaller

than the terms on the left-hand side and so is neglected. At $r = r_0$, (2.2)–(2.4) become

$$\omega_i u(r_0) - 2\Omega v(r_0) = 0 \tag{2.5}$$

$$\omega_i\left(\alpha + \frac{n^2}{\alpha r_0^2}\right)v(r_0) + \frac{1}{r_0}[\alpha D\Gamma(r_0) + nDW(r_0)]u(r_0) = 0 \tag{2.6}$$

where $\omega \equiv \omega_r + i\omega_i$ and $\omega_r \equiv W(r_0)\alpha - \Omega(r_0)n$.

At $r = r_0$ the surfaces of constant phase are assumed to be interleaving helical sheets that have a normal vector with no radial component. If such a radius is to exist, then certainly a necessary condition is that the normal vector to these sheets is not tilted into the radial direction by the shear of the mean velocity at r_0. If that were to happen, then the length scale of radial variation would not be sufficiently small to justify (2.5) and (2.6). So, there can be no radial derivative near r_0 of the rate of advection of a perturbation quantity like $\ln|u'|$,

$$\frac{\partial}{\partial r}\left(W\frac{\partial}{\partial z} + \Omega\frac{\partial}{\partial \theta}\right)\ln|u'| = 0. \tag{2.7}$$

Therefore, we are restricted to considering modes with

$$\frac{\alpha}{n} = \frac{D\Omega(r_0)}{DW(r_0)}. \tag{2.8}$$

The above is equivalent to restricting the slope of the helical surfaces of constant phase to be parallel to the shear vector of the mean velocity at r_0.

We assume a continuous spectrum of modes exist; for any value of r_0, (2.5), (2.6) and (2.8) can be solved for the eigenvalue and eigenvector. As shown in LS, r_0 is the radius where the magnitude of u has a local maximum and it is where centrifugal exchange of fluid may occur unimpeded by counteracting perturbation pressure forces. The region near r_0 is the energy source of an unstable mode. The growth rate of large wavenumber helical instability is ω_i where

$$\omega_i^2 = \frac{-2VD\Omega[D\Gamma D\Omega + (DW)^2]}{[r_0^2(D\Omega)^2 + (DW)^2]}, \tag{2.9}$$

evaluated at any r_0. The vortex will be unstable if at some radius

$$VD\Omega[D\Gamma D\Omega + (DW)^2] < 0. \tag{2.10}$$

If $DW = 0$, then $D\Gamma^2 > 0$ is necessary for stability, and, therefore, V and Ω cannot change sign (Drazin and Reid 1982, p. 78). The vortex is stable to vertical or two-dimensional disturbances if $D\zeta^2 < 0$ (Drazin and Reid 1982, p. 81). In a vortex where $D\Gamma^2 > 0$ and $D\zeta^2 < 0$, as in (1.2), then $VD\Omega < 0$ and $D\Gamma D\Omega < 0$, and instability occurs if $(DW)^2$ is sufficiently large.

The growth rate (2.9) is determined only by local conditions, and so is analogous to the Brunt-Väisälä frequency. Large-wavenumber helical instability is a conventional parcel instability in that the restoring force due to the perturbation pressure does not play a role. [This fact was implicitly assumed in Emanuel (1984).] The mechanism of the instability is therefore easily illustrated. Consider a Q-vortex with q taken to be positive. The shear vector points in the negative $\hat{\mathbf{k}}$ and negative $\hat{\theta}$ direction. Figure 1 is a close-up view, looking towards the axis, at a surface of constant r. Nodal lines are shown separating regions of positive u' from negative u'. The tendency of the vorticity tilting terms in (2.3) is indicated schematically (of course the tendencies are actually superposed). Tilting of vertical vorticity always tends to make $u'v' < 0$, whereas $u'v' > 0$ is what is needed if centrifugal forces are to overcome the inward mean pressure forces when u' is positive and vice versa when u' is negative. The correlation $u'v' > 0$ is precisely what is provided by tilting of azimuthal vorticity. Therefore, with sufficient azimuthal vorticity, or $(DW)^2$, a centrifugal instability is possible.

Although (2.10) is not a necessary condition for instability, I will assume it serves as a close approximation to the necessary condition. For example, the Q-vortex is known to be unstable for q as large as 1.58 for $n = 1$ (Leibovich 1984), whereas (2.10) indicates stability for $q > 1.41$. Leibovich (1984) suggests that (2.10) is a criterion for massive instability and transition to turbulence at large Reynolds number. I will follow the lead of Stewartson and Leibovich (1987) and treat (2.10) as a necessary and sufficient condition for being

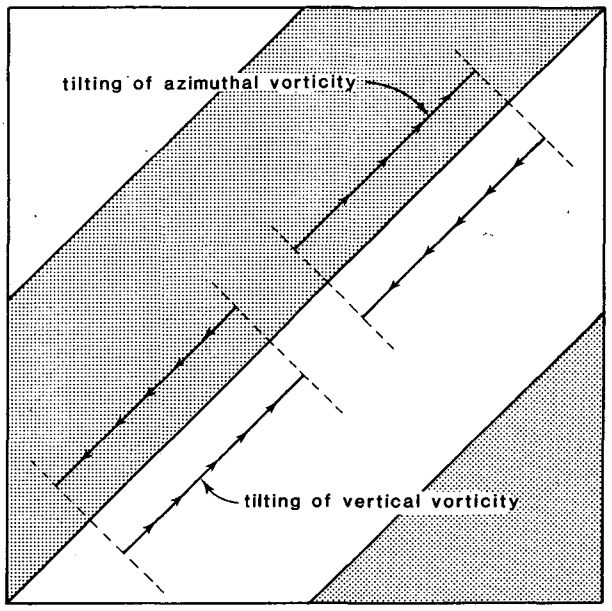

FIG. 1. A small portion of a surface of constant r in a Q-vortex; V is to the right, W upward. Nodal lines separate regions of outward velocity u' (stippled) from regions of inward velocity. The tendencies of the circulations induced by tilting of vertical vorticity and azimuthal vorticity are indicated.

"strongly unstable." For brevity, conditions in which (2.10) is not satisfied will be referred to as being "stable" conditions, leaving unstated the qualification of possible weak instability at small wavenumbers.

3. Some particular solutions for loss-free, columnar vortices

A loss-free, incompressible columnar vortex in cyclostrophic balance obeys

$$\frac{d}{dy}\frac{\Gamma^2}{2} + y\frac{dW^2}{dy} = 0 \tag{3.1}$$

where $y \equiv r^2/2$. Here loss-free means that the head or Bernoulli constant has the same value throughout the flow. This assumption is appropriate for a steady flow which is nearly stagnant far from the core and for which the flow into the core occurs without significant dissipation. For $VD\Omega < 0$, the vortex is unstable to large-wavenumber, helical instability if

$$D\Gamma D\Omega + (DW)^2 > 0 \tag{3.2}$$

at any r. Using W as the independent variable, (3.1) is

$$\frac{d}{dW}(\Omega y) = -\frac{W}{2\Omega} \tag{3.3}$$

and (3.2) is

$$2\frac{d\Omega}{dW}\frac{d}{dW}(\Omega y) > -1. \tag{3.4}$$

The above, taken together give a sufficient condition for instability in loss-free vortices:

$$\frac{W}{\Omega}\frac{d\Omega}{dW} < 1. \tag{3.5}$$

The marginally stable solution is

$$\Omega = \sqrt{b/2}W, \tag{3.6}$$

and from (3.3),

$$W = \frac{a}{1+by} \tag{3.7}$$

where a and b are arbitrary constants.

A solution to

$$\phi_{yy} - \left[\frac{1}{W}W_{yy} - \frac{\Gamma}{2y^2W^2}\Gamma_y\right]\phi = 0 \tag{3.8}$$

with $\phi(0) = 0$ and $\phi_y(0)$ arbitrary determines whether or not the flow in a columnar vortex is supercritical to axisymmetric waves (Benjamin 1962). If the solution for the test function $\phi(y)$ vanishes for some $y > 0$ in the domain, then the flow is subcritical; otherwise, it is supercritical. If the flow is loss-free, then (3.1) and (3.8) gives a simpler equation for testing criticality:

$$\phi_{yy} - \left[\frac{1}{Wy}\frac{d}{dy}\left(y\frac{dW}{dy}\right)\right]\phi = 0. \tag{3.9}$$

A columnar vortex will be stable to axisymmetric disturbances (of arbitrary vertical wavenumber) if

$$\frac{\dfrac{d\Gamma^2}{dy}}{y^2\left(\dfrac{dW}{dy}\right)^2} > 1 \tag{3.10}$$

for all y (Howard and Gupta 1962). If the flow is loss-free, then a necessary condition for axisymmetric instability is

$$\frac{y}{W}\frac{dW}{dy} < -4 \tag{3.11}$$

for some y. A similar sufficient condition for large-wavenumber, helical instability in a loss-free vortex can be derived from (3.1) and (3.2):

$$\frac{y}{W}\frac{dW}{dy} < -\left(1 + \frac{W^2}{V^2}\right)^{-1}, \tag{3.12}$$

or just

$$\frac{y}{W}\frac{dW}{dy} < -1 \tag{3.13}$$

for some y. In a loss-free columnar vortex, large-wavenumber helical modes will always be unstable if axisymmetric modes are unstable.

The marginally stable solution in (3.7) can be generalized into a family of vortex profiles:

$$W(y) = a(1+by)^{-\beta} \tag{3.14}$$

where $\beta > 0$. By (3.13), the vortex is unstable to large-wavenumber helical modes if $\beta > 1$. By (3.11), the vortex could be unstable to axisymmetric modes only if $\beta > 4$. The vortex could be unstable to two-dimensional disturbances only if $\beta > 1$. Numerical integration of (3.9) shows the vortex is supercritical for all $\beta > 0$. This last result should be contrasted with the Q-vortex with $W_\infty = 0$. Integration of (3.8) shows that all such Q-vortices are subcritical, as mentioned in the Introduction.

The vortex velocity profiles $W(r)$ and $V(r)$ can be related to the terminal (i.e., adjacent to the vortex core) vertical profiles of radial velocity U and V in the end-wall boundary layer (Rotunno 1980; FR). A stream function $\psi(r, z)$ for the meridional flow is defined as

$$U = \frac{1}{r}\frac{\partial\psi}{\partial z} \tag{3.15}$$

and

$$W = -\frac{1}{r}\frac{\partial \psi}{\partial r}. \tag{3.16}$$

Burggraf et al. (1971) show that the terminal boundary layer under a potential vortex is nearly loss-free for large Re:

$$r^2U^2 + \Gamma^2 = \Gamma_0^2, \tag{3.17}$$

except in a shallower viscous sublayer where the relative depth vanishes as $\mathrm{Re} \to \infty$. This is also clearly demonstrated in Wilson and Rotunno (1986). Using (3.17), the Reynolds number for the meridional flow in the corner region (where the radial boundary-layer flow turns into the axial core flow) is easily shown to be Re. Therefore, Γ is conserved along steady stream surfaces in the corner region as $\mathrm{Re} \to \infty$.

In the marginally stable vortex solution of (3.6) and (3.7),

$$\Gamma = \frac{\sqrt{2b}ay}{1 + by}. \tag{3.18}$$

In a dimensionless solution where $\Gamma(\infty) = 1$,

$$b = 2a^2. \tag{3.19}$$

From (3.16) and (3.7),

$$\psi = -\frac{1}{2a}\ln(1 + 2a^2y), \tag{3.20}$$

and therefore

$$\Gamma = 1 - e^{2a\psi} \tag{3.21}$$

both within the vortex and the terminal boundary layer. Using (3.21) in (3.17) gives a differential equation for $\psi(z)$ in the boundary layer

$$\left(\frac{d\psi}{dz}\right)^2 + (1 - e^{2a\psi})^2 = 1 \tag{3.22}$$

with solution

$$e^{2a\psi} = \frac{2}{1 + (1 + 2az)^2}. \tag{3.23}$$

Using (3.23) in both (3.21) and (3.22) will give the vertical profiles for Γ and rU in the terminal boundary layer. Before considering this solution further, and the physical conditions required to produce it, two other particular solutions will be derived, for comparison, for loss-free, end-wall vortices and their corresponding boundary layers.

First, consider a profile for W similar to that in (1.2b):

$$W = ae^{-by}. \tag{3.24}$$

From (3.1), the corresponding loss-free profile for Γ is

$$\Gamma^2 = \frac{a^2}{b}(1 - e^{-2by}) - 2ya^2e^{-2by}. \tag{3.25}$$

I will call (3.24) and (3.25) the loss-free Q-vortex. From (3.9), this profile is supercritical. In a dimensionless solution where $\Gamma(\infty) = 1$,

$$a^2 = b. \tag{3.26}$$

From (3.16) and (3.24),

$$\psi = \frac{1}{a}(e^{-a^2y} - 1) \tag{3.27}$$

and therefore

$$\Gamma^2 = 1 - [1 - 2\ln(1 + a\psi)](1 + a\psi)^2. \tag{3.28}$$

Using (3.28) in (3.17) gives a differential equation for $\psi(z)$ in the boundary layer that can be solved numerically.

Secondly, consider the solution for the loss-free Burggraf boundary layer and the corresponding end-wall vortex. The boundary-layer solutions in Burggraf et al. (1971) were made dimensionless using Γ_0 as the circulation scale and δ as the length scale. Their numerical solution for the terminal profile of rU in the limit $\mathrm{Re} \to \infty$ is listed in a table in their paper. A cubic spline was filled to that solution and $\Gamma(\psi)$ calculated using (3.17).

In the loss-free Burggraf boundary layer, ψ decreases from $\psi = 0$ at the lower boundary to about $\psi = -1.2$ as $z \to \infty$. So, for purposes of comparison, $a = 1/1.2$ in (3.27) so that $\psi = -1.2$ as $y \to \infty$ in the loss-free Q-vortex. In (3.20), $\psi \to -\infty$ as $y \to \infty$. So, in (3.20), $a = 0.943$, which makes the lowest part of the boundary layer to the marginally stable vortex correspond well to the lowest part of the loss-free Burggraf boundary layer. The three sets of boundary-layer profiles are plotted in Fig. 2. The boundary layer to the loss-free Q-vortex can well represent the loss-free Burggraf boundary layer. The boundary layer to the marginally stable vortex can represent the loss-free Burggraf boundary layer only up to about $z = 0.7$, but then for larger z it departs significantly.

The corresponding sets of vortex profiles are plotted in Fig. 3. The loss-free Burggraf vortex has been computed by the method described in FR. The growth rate of large-wavenumber helical instability calculated from (2.9) is plotted in Fig. 4. The loss-free Q-vortex and the loss-free Burggraf vortex have very similar stability properties, although, at first sight, the actual vortex profiles do not seem to match each other any better than they match the loss-free, marginally stable vortex. In fact, a Q-vortex with $q = 0.86$ and $W_\infty = 0$ (Fig. 5) is a satisfactory representation of the loss-free Q-vortex and has nearly the same maximum growth rate of the instability (Fig. 6). However, no Q-vortex could sat-

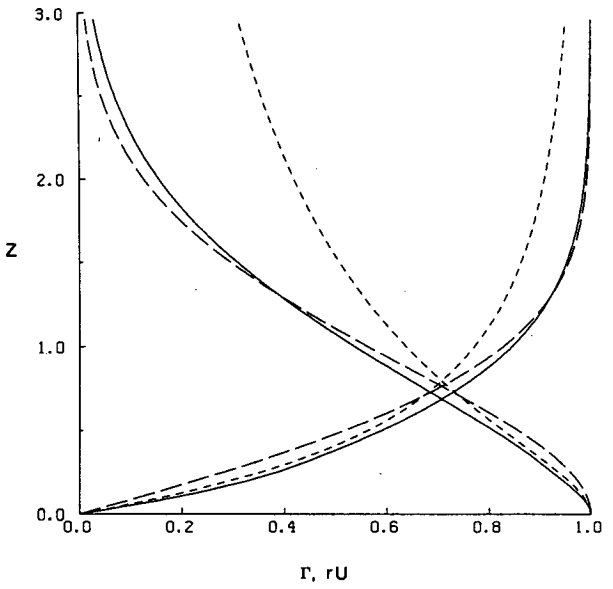

FIG. 2. The terminal boundary layer profiles of $\Gamma(z)$ and $rU(z)$: solid curve, loss-free Burggraf boundary layer; long dashed curve, loss-free Q-vortex; short dashed curve, loss-free, marginally stable vortex. $\Gamma(0) = 0$.

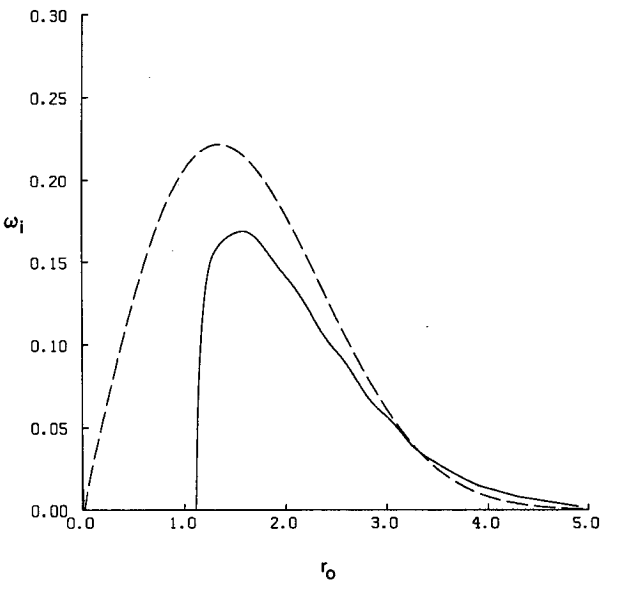

FIG. 4. The growth rate of large-wavenumber, helical instability as a function of r_0 for the vortices in Fig. 3: solid curve, loss-free Burggraf vortex; dashed curve, loss-free Q-vortex.

isfactorily represent the profiles, stability, and supercriticality of the marginally stable vortex.

Significantly, all the unstable vortices have similar steepness to $W(r)$ at large r. It is obvious from (3.2) that decreasing $|DW|$ while maintaining the magnitude of $|W|$ would tend to stabilize an end-wall vortex and yet retain its supercriticality. It is not so obvious that this remedy should have been effective in loss-free vortices. By (3.1), if $|DW|$ is decreased, then so is $|D\Gamma|$, and a decrease in $|D\Gamma|$ is destabilizing.

From these results it is concluded tentatively that a sufficiently slow approach of $\Gamma(z)$ to its asymptotic value $\Gamma(\infty)$ in a loss-free boundary layer renders the end-wall vortex stable to large-wavenumber modes. Conceivably, an eddy diffusivity that increases with height could produce such a tendency in $\Gamma(z)$. How-

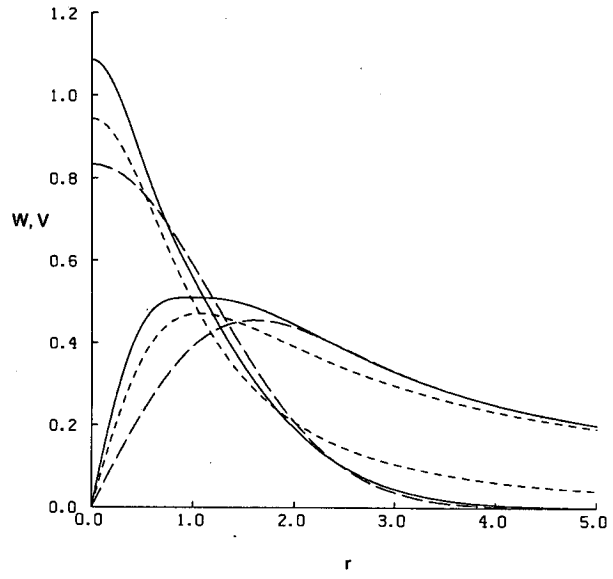

FIG. 3. Vortex profiles $W(r)$ and $V(r)$: solid curve, loss-free Burggraf vortex; long dashed curve, loss-free Q-vortex; short dashed curve, loss-free, marginally stable vortex; $V(0) = 0$.

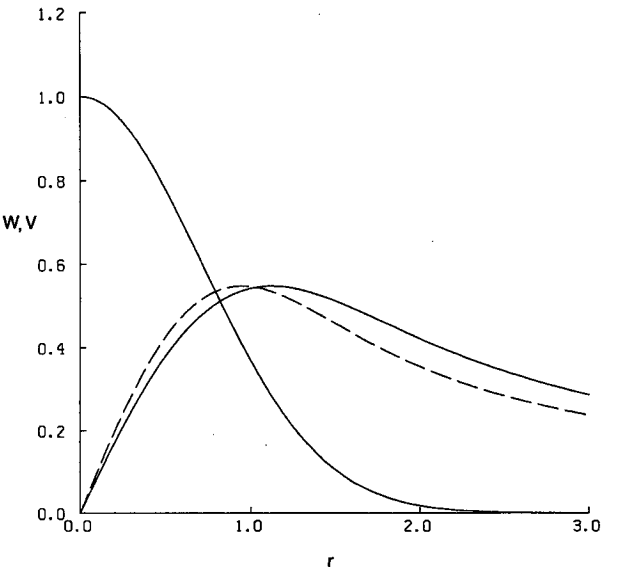

FIG. 5. Vortex profiles $W(r)$ and $V(r)$: solid curve, Q-vortex with $q = 0.86$ and $W_\infty = 0$; dashed curve, loss-free profile for $V(r)$.

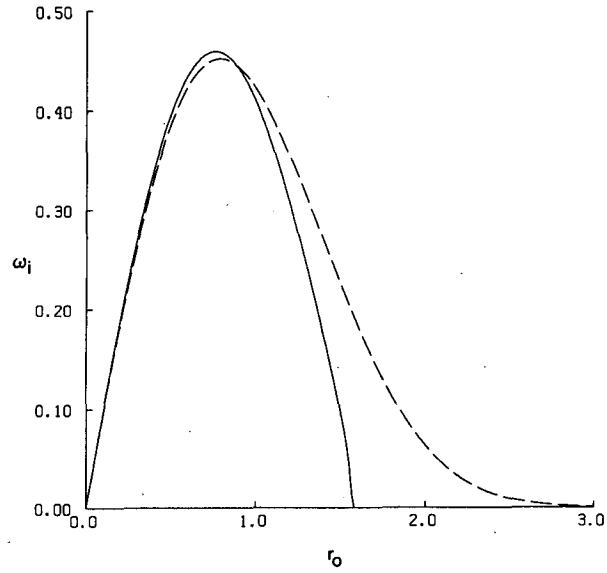

FIG. 6. The growth rate of large-wavenumber, helical instability as a function of r_0 for the vortices in Fig. 5. Solid curve, Q-vortex with $q = 0.86$ and $W_\infty = 0$; dashed curve, for a vortex with the same $W(r)$ but with the loss-free profile for $V(r)$.

ever, if the end-wall boundary layer is turbulent, it will not be loss-free. So, I have difficulty in suggesting any natural processes that would actually produce a boundary layer like that of the loss-free, marginally stable vortex. In the next section it will be shown how end-wall boundary layers with some loss of head can produce stable, supercritical end-wall vortices, even without the described tendency in $\Gamma(z)$.

4. A marginally stable vortex with some loss of head

In the end-wall boundary layer under a potential vortex, significant head loss occurs only in the viscous sublayer with a terminal depth of order $\delta\ \mathrm{Re}^{-1/2}$ as $\mathrm{Re} \to \infty$ (Burggraf et al. 1971). As the viscous sublayer turns through the corner into the vortex core, it has a tendency to produce a velocity defect, or reduced axial velocity, right on the core axis. However, it can be easily shown that such a velocity defect would suffer significant diffusion before being advected downstream a distance δ. Indeed, the laser-Doppler anemometry (LDA) measurements of Escudier et al. (1982) show apparently supercritical vortices (their classes A and B) in which no velocity defect survives past the corner region. Escudier et al. (1980) state that the resolution of the LDA instrument prevents the velocity defect from being seen throughout the cores. This explanation is not supported by the numerical simulation of Wilson and Rotunno (1986), in which no velocity defect survives past the corner region of the simulated supercritical, end-wall vortex.

The loss of head that was originally confined to the viscous sublayer is therefore diffused somewhat throughout the inner core of an end-wall vortex. I will use $\Gamma(\psi)$ from (3.28) in a simple experiment exploring the effect of such head loss on the stability and criticality of the end-wall vortex. If the vortex is marginally stable, $w(\psi)$ can be obtained from (3.2):

$$\frac{dw}{d\psi} = \left[-\frac{1}{2y}\frac{d\Gamma}{d\psi}\left(\frac{d\Gamma}{d\psi} + \frac{1}{yw}\Gamma\right)\right]^{1/2}. \tag{4.1}$$

The above has been solved by a shooting scheme with boundary condition $w \to 0$ as $y \to \infty$, concomitantly with

$$\frac{dy}{d\psi} = -\frac{1}{w}. \tag{4.2}$$

Loss of head $H(\psi)$ is imposed in the solution by the constraint of marginal stability. The head in the solution is solved for by

$$\frac{dH}{d\psi} = w\frac{dw}{d\psi} + \frac{\Gamma}{2y}\frac{d\Gamma}{d\psi} \tag{4.3}$$

(e.g., FR; Rotunno, 1980) with a boundary condition $H(0) = 0$. The resulting vortex profiles $W(r)$, $V(r)$, and $H(r)$ are shown in Fig. 7. For comparison, the loss-free vortex profiles for the same $\Gamma(\psi)$ are also plotted. The criticality test in (3.8) can be transformed to one with ψ as the independent variable rather than y (FR). The test shows that the marginally stable profile in Fig. 7 is supercritical. The stable, supercritical profiles in Figs. 3 and 7 should be contrasted with the rather restricted class of unstable, subcritical vortices studied by Staley and Gall (1984).

The solution in Fig. 7 serves as an example that if a

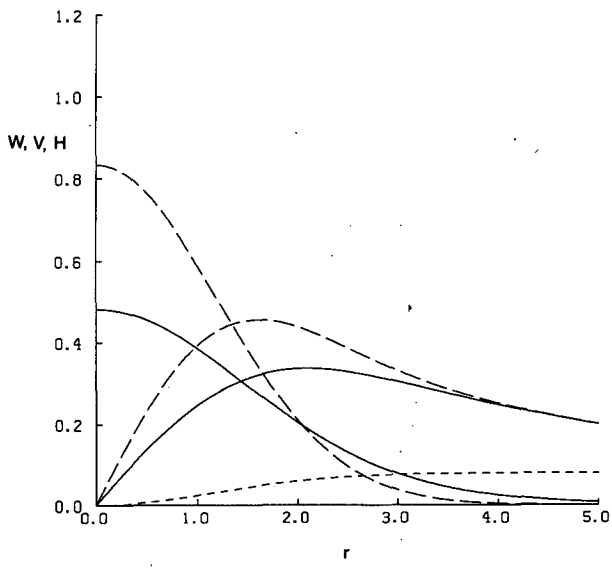

FIG. 7. Vortex profiles $W(r)$ and $V(r)$ for two vortices with $\Gamma(\psi)$ from Eq. (3.28): long dashed curve, the loss-free Q-vortex with H = constant; solid curve, a marginally stable vortex with $H(\psi)$ as indicated by the short dashed curve.

moderate amount of dissipation occurs throughout an end-wall boundary layer, then the end-wall vortex can be both supercritical and stable to large-wavenumber helical instabilities. In this case the maximum loss of head on the axis is 0.078. This loss of head is smaller than what one might infer by simply looking at the velocity profiles. Without a change in pressure, this loss of head would have reduced the maximum axial velocity from 0.83 to 0.73. So, most of the reduction in the axial velocity apparent in Fig. 7 is an indirect effect of dissipation and is associated with an increase in pressure due to the broadening of the core.

5. Conclusion

The purpose of this paper was to establish theoretical evidence that supercriticality and stability are not mutually exclusive in end-wall vortices formed at high Reynolds number. Therefore, smooth laboratory vortices like the one pictured in FR, and smooth geophysical vortices like the waterspouts pictured in Golden (1974) may be dynamically similar, though, as yet, there is no incontrovertible evidence for this. If they are similar, then most numerical simulations of geophysical vortices, which use large values of eddy viscosity, have not been well suited to model them (see Howells et al. 1988 and references therein). The inviscid analysis in FR would be more suitable.

The existence of laminar geophysical vortices at first seems paradoxical. Locally, many geophysical vortices appear axisymmetric. A truly laminar, axisymmetric boundary layer at $\mathrm{Re} = 10^8$ should be well modeled by the loss-free Burggraf boundary layer. The resulting vortex should be supercritical but unstable. The paradox is resolved by recognizing that the end-wall boundary layer itself is turbulent at sufficiently large Re (Phillips and Khoo 1987). A turbulent boundary layer could lose sufficient head and produce a stable, supercritical end-wall vortex as in the solution in section 4. Such loss of head can be seen, for example, in the numerical solutions of end-wall boundary layers in Prahlad and Head (1978). I conclude that supercritical end-wall vortices can be stable at either sufficiently large or sufficiently small Reynolds number. Either extreme could produce the required loss of head. However, excessive loss of head, perhaps due to a rough boundary, would render the vortex subcritical and hence, probably turbulent.

Experimental evidence for laminar flow in geophysical vortices is circumstantial. The many observations of geophysical vortices (tornadoes, waterspouts, dust devils) reveal that some are unquestionably turbulent. Some geophysical vortices though appear to be smooth and perhaps laminar. Perhaps the level of turbulence is just low in the smooth vortices, but then there does not appear to be a continuous gradation of appearances from the smooth to the turbulent variety. Likewise, there are very few direct measurements of the axial flow in geophysical vortices and therefore experimental evidence for supercriticality is also circumstantial.

Finally, I reiterate some of the drawbacks in modeling columnar vortices as Q-vortices. First, if (1.2) is used to model a supercritical end-wall vortex, then W_∞ cannot be taken as exactly zero. A better choice would be to use the loss-free Q-vortex in (3.24) and (3.25), or at least a loss-free outer solution. Secondly, there is a danger in fitting a Q-vortex to experimental vortices by simply using

$$q = 1.56 V_{\max} / \Delta W \tag{5.1}$$

where $V_{\max}$ is the maximum azimuthal velocity and ΔW is the axial velocity difference between the axis and the outer flow, as was done, for example, in Escudier et al. (1982). Such a fit to the marginally stable solutions of sections 3 and 4 would indicate that the vortices were strongly unstable. At least in those cases, the conditions for instability are too subtle to diagnose by means other than (2.10).

REFERENCES

Benjamin, T. B., 1962: Theory of the vortex breakdown phenomenon. *J. Fluid Mech.*, **14**, 593–629.

Burggraf, O. R., K. Stewartson and R. Belcher, 1971: Boundary layer induced by a potential vortex. *Phys. Fluids*, **14**, 1821–1833.

Drazin, P. G., and W. H. Reid, 1982: *Hydrodynamic Stability*. Cambridge University Press, 527 pp.

Emanuel, K. A., 1984: A note on the stability of columnar vortices. *J. Fluid Mech.*, **145**, 235–238.

Escudier, M. P., J. Bornstein and N. Zehnder, 1980: Observations and LDA measurements of confined turbulent vortex flow. *J. Fluid Mech.*, **98**, 49–63.

——, —— and T. Maxworthy, 1982: The dynamics of confined vortices. *Proc. Roy. Soc. London*, **382A**, 335–360.

Fiedler, B. H., and R. Rotunno, 1986: A theory for the maximum windspeeds in tornado-like vortices. *J. Atmos. Sci.*, **43**, 2328–2340.

Golden, J. H., 1974: The life cycle of Florida Keys' Waterspouts. I. *J. Appl. Meteor.*, **13**, 676–692.

Howard, L. N., and A. S. Gupta, 1962: On the hydrodynamic and hydromagnetic stability of swirling flows. *J. Fluid Mech.*, **14**, 463–476.

Howells, P., R. Rotunno and R. K. Smith, 1988: A comparative study of atmospheric and laboratory-analogue numerical tornado-vortex models. *Q. J. Roy Meteor. Soc.*, **114**, 801–822.

Leibovich, S., 1984: Vortex stability and breakdown: Survey and extension. *AIAA J.*, **22**, 1192–1205.

——, and K. Stewartson, 1983: A sufficient condition for the instability of columnar vortices. *J. Fluid Mech.*, **126**, 335–356.

Lessen, M., and F. Paillet, 1974: The stability of a trailing line vortex. Part 2: Viscous theory. *J. Fluid Mech.*, **65**, 769–779.

Phillips, W. R. C., and B. C. Khoo, 1987: The boundary layer beneath a Rankine-like vortex. *Proc. Roy. Soc. London*, **411A**, 177–192.

Prahlad, T. S., and M. R. Head, 1976: Numerical solutions for boundary layers beneath a potential vortex. *Comput. Fluids*, **4**, 157–169.

Rotunno, R., 1980: Vorticity dynamics of a convective swirling boundary layer. *J. Fluid Mech.*, **97**, 623–640.

Staley, D. O., and R. L. Gall, 1984: Hydrodynamic instability of small eddies in a tornado vortex. *J. Atmos. Sci.*, **41**, 422–429.

Stewartson, K., and S. Leibovich, 1987: On the stability of a columnar vortex to disturbances with large azimuthal wavenumber: The lower neutral points. *J. Fluid Mech.*, **178**, 549–566.

Wilson, T., and R. Rotunno, 1986: Numerical simulation of a laminar end-wall vortex and boundary layer. *Phys. Fluids*, **29**, 3993–4005.